Hazard and risk of the Moosehide Slide (Ëddhà dädhëchą), Dawson City, Yukon

M. Sturzenegger, M. Jakob, L.U. Arenson, A. Mitchell, J. Harrington & B. Collier-Pandya
BGC Engineering, Vancouver, British Columbia, Canada
M. Ondercin
BGC Engineering, Toronto, Ontario, Canada
N. Suszek
BGC Engineering, Calgary, Alberta, Canada
J. Bond
Yukon Geological Survey, Whitehorse, Yukon, Canada

GeoCalgary 2022 October 2-5
Reflection on Resources

ABSTRACT
The Moosehide Slide is a rockslide located on the northern margins of Dawson City, Yukon. It features a prominent headscarp, corresponding to the initiation zone of a pre-historic landslide. Field evidence, such as tension cracks and tension-split trees, and airborne lidar change detection analysis indicate retrogressive instability in the headscarp zone. This paper summarizes the steps completed to quantify landslide hazard and risk associated with a potential rock avalanche with possible runout to the north end of Dawson City. The steps completed include i) quantification of potential source volumes and hazard probabilities at the headscarp; ii) modelling of the rock avalanche runout characteristics; iii) assessment of the influence of permafrost degradation on the likelihood and intensity of the rock avalanche; and iv) quantitative risk assessment in both existing and potential future developments at the north end of Dawson City. The results are integrated in two types of maps for communication of landslide hazard and risk to the public and decision makers. These maps form the basis for the development of a monitoring program and emergency response plan to mitigate life-loss risk in existing developments.

RÉSUMÉ
Le Moosehide Slide est un glissement de terrain qui se trouve en marge de Dawson City, Yukon. Il est défini par une cicatrice qui correspond à la zone de rupture d'un glissement de terrain préhistorique. Des observations de terrain, comme des fractures et troncs d'arbres déchirés, et une analyse de données lidar indiquent que des mouvements rétrogressifs sont en cours dans la zone de rupture du glissement préhistorique. Cet article présente les analyses qui ont été faites pour quantifier le danger et le risque associés à un éboulement qui pourrait impacter la partie nord de Dawson City. Ces analyses comportent i) l'estimation du volume des instabilités et leur probabilité d'occurrence; ii) la modélisation de l'éboulement; iii) une étude de l'influence de la dégradation du pergélisol sur la probabilité d'occurrence et l'intensité de l'éboulement; et iv) la quantification du risque dans les constructions existantes et futures dans la partie nord de Dawson City. Les résultats sont intégrés dans deux types de cartes pour communiquer le danger et le risque au public et aux décideurs. Ces cartes forment une base pour l'élaboration d'un système de surveillance et d'un plan d'urgence pour réduire le risque de décès dans les constructions existantes.

1 INTRODUCTION

The Moosehide Slide, also known as Ëddhà dädhëchą, is located at the north end of Dawson City, Yukon, on the east bank of the Yukon River, some 2 km downstream of the confluence of the Klondike River (Figure 1). It features a prominent headscarp, interpreted as the initiation zone of a pre-historic landslide (Brideau et al. 2007a). The debris of the landslide extends from the base of the headscarp to the Yukon River and includes a rock glacier in the central portions (Brideau et al. 2007b), which has transitioned into an earthflow in the lower parts.

First Nation's oral history points towards a rockslide event at the location of the Moosehide Slide, initiated by members of a local tribe, and which buried and killed all members of a rival tribe (Sokolovski 2020; YukonInfo.com/moose-hide-slide). The pre-historic landslide may have initiated in igneous rocks of the Slide Mountain terrane, at or near a zone where they are in contact with the underlying Klondike Schist of the Yukon-Tanana terrane (Green 1972; Brideau et al. 2007a). Hughes (1979) identified weathered angular debris in a borrow pit in the lower section of the debris deposit, overlain by 25 cm of organic material, which in turn is covered by 6.5 m of fresh angular debris. The organic material provided a radiocarbon age of 1,740 years BP. A possible interpretation was that the weathered, angular debris identified below the organic material corresponds to the pre-historic landslide, overgrown by a forest that was eventually overridden by a rock glacier or earthflow. It is still unclear if the debris corresponds to a pre-historic rock avalanche reaching the Yukon River or the debris of smaller landslide event(s) in the upper part of the slope, which was subsequently re-mobilized by the rock glacier and/or earth flow.

Brideau et al. (2007a) studied the failure and triggering mechanisms of the pre-historic slide. A kinematic analysis of discontinuity data collected in the field did not identify a simple failure mechanism. Considering the heavily fractured rock mass conditions, the failure mechanism of this pre-historic event was therefore interpreted to be sliding along a pseudo-circular failure surface. The slide may have been triggered by a combination of high pore-water pressures and seismic loading.

The headscarp of the pre-historic slide is subject to further instabilities. Detachments of the retrogressing source material may generate a rock avalanche with possible runout to Dawson City. The Yukon Geological Survey has been asked by the Department of Community Services to assist in assessing the life-loss and economic risk to both existing and potential residential developments of the northern portions of Dawson City. A comprehensive study of the Moosehide Slide was completed, in accordance with modern landslide risk management practice used in Canada (VanDine 2012).

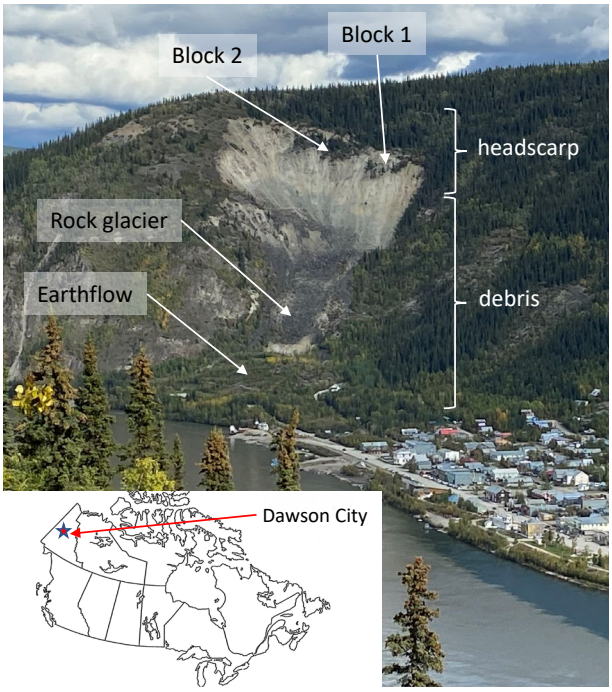

Figure 1. North end of Dawson City and main features of the Moosehide Slide. Photo by M. Sturzenegger.

This paper summarizes the results of the Moosehide Slide study in which we integrate various quantitative tools to assess landslide risk and inform risk reduction strategies, such as zoning and monitoring. The quantitative tools include i) airborne lidar scanning (ALS) change detection and the sloping local base level (SLBL) for quantification of potential landslide source volumes; ii) geothermal modelling to assess the effect of climate change and permafrost degradation on rock avalanche volume and runout characteristics; iii) 3D modelling for the simulation of potential rock avalanche runout extent and intensity; and iv) generation of both composite hazard and risk maps. The maps serve as key communication tools with the public and decision makers, and to inform risk management strategies.

2 HAZARD QUANTIFICATION AND MAPPING TOOLS

2.1 Landslide Source Identification and Volume Estimation

Landslide scenarios are defined based on a combination of ALS change detection analysis, field observations and SLBL analysis.

The ALS change detection analysis involves comparison of 2013, 2018 and 2020 ALS datasets. The bare earth lidar datasets are analyzed for topographical change with the software program PolyWorks (InnovMetric 2020) using a conventional methodology (Abellan et al. 2009; Oppikofer et al. 2009; Lato et al. 2015). The steps include (1) alignment to minimize the differences between sequential scans; (2) definition of the limit of detection (LoD) defined as the 2.5% and 97.5% cumulative model differences between the non-changing regions of the ALS datasets, (3) 3-dimensional (3D) shortest distance change analysis.

Based on the interpretation that the failure surface of the pre-historic Moosehide Slide was pseudo-circular, we assume that a potential retrogressive failure would also follow a pseudo-circular failure surface. The potential failure volumes are estimated using the SLBL concept (Jaboyedoff et al. 2004; 2019), which allows definition of pseudo-circular failure surfaces. The concept is similar to the geomorphological concept of “base level” but is applied to a slope corresponding to the source zone of a landslide (as opposed to the horizontal).

2.2 Numerical Geothermal Modelling for Permafrost Degradation

Permafrost and its climate-change-related degradation is hypothesized to influence volumes associated with a potential rock avalanche by progressive active layer thickening. If a rock mass in the source area of the Moosehide Slide were to fail, it can preserve its mass or entrain additional sediment on its descent, adding to its volume and mass. Geophysical imaging of the rock glacier below the Moosehide Slide headscarp suggests that much of the slide debris is frozen, with an active layer thickness, i.e., the seasonally unfrozen layer, between 3 m and 5 m (Brideau et al. 2015; J. Coates, pers. communication). As temperatures increase, the active layer thickens. If the landslide occurs during the summer months a several metre-thick active layer could be entrained and added to the total landslide volume.

To test the hypothesis and, its impact on material entrainment potential and potentially the stability of the rock mass, we numerically model the geothermal regime. The numerical geothermal model of the Moosehide Slide is developed using TEMP/W (Version 10.2.1.19666), a commercially available finite-element heat conduction model that can account for phase change and latent heat flux. The model assumes that the heat flow occurs

primarily as vertical conduction, a reasonable approach for areas with modest topographic relief, such as the Moosehide Slide debris.

2.3 Rock Avalanche Runout Modelling

The potential rock avalanche runout extent and intensity (i.e., depth and velocity) are estimated using the program DAN3D (McDougall & Hungr 2004). The sliding surface used for the runout modelling is based on ALS data and the basal rupture surface geometry estimated from the SLBL analysis results (Figure 2).

A rock avalanche is defined as extremely rapid, massive, flow-like motion of fragmented rock from large rockslides, rockfalls or rock collapses (Hungr et al. 2014). The transition to the rock avalanche type of flow motion may occur for volumes ranging between 100,000 m^3 and 1,000,000 m^3 (Corominas 1996), and results in excess runout distance (travel angle less than 31°) in comparison to typical rockfall or rock collapse debris modes of deposition. The runout analysis presented here accounts for this by using different flow models as a function of block volume scenarios. Based on experience with runout model calibrations for similar cases, the frictional model governed by the friction angle (φ) between the sliding mass and the sliding surface provides a realistic representation of the runout resulting from the failure of Block 1 and 2 scenarios (see Table 1). In comparison, the Voellmy flow resistance model is more appropriate for larger failure volumes (McDougall 2017), such as Block 3 and 4 scenarios. The Voellmy model is governed by two parameters: a friction coefficient, f; and a turbulence coefficient, ξ, which produces a velocity-dependent resistance that tends to limit flow velocities (similar to air drag acting on a falling object) (McDougall & Hungr 2004).

2.4 Hazard and Risk Mapping

Two types of maps are created. A composite hazard map is generated based on the integration of both landslide annual hazard probability estimates and runout modelling results. A risk map is created considering consequence parameters (i.e., temporal probability, vulnerability, and exposure).

2.4.1 Composite Hazard Map

The procedure to generate a composite hazard map is to first create individual hazard maps for a series of representative hazard scenarios, and then to overlay them to display the maximum runout extent of all scenarios and highlight zones with greater hazard probability or intensity (Jakob et al. 2022).

For each individual hazard map, an impact intensity probability (P_I) geohazard mapping scheme is created that consists of two main components: the intensity expressed by an impact force per metre flow width and the probability of the respective events. The underlying equation is:

$$P_I = v^2 \times \rho_f \times d_f \times P(H) \quad [1]$$

where v is flow velocity (m/s), d_f is the fluid's flow depth (m), ρ_f is the fluid or particle density (kg/m^3) to obtain a unit of force per metre flow width for the three left terms in Equation 1. $P(H)$ is the annual probability of the geohazard. The unit of P_I is Newton per metre per year (N/m per yr).

With only limited data to constrain the annual hazard probability for each scenario, order of magnitude estimates are used, and upper and lower bound maps created. Flow velocity and depth are outputs from the runout modelling.

When overlaying individual hazard maps, weighting factors are assigned to different runout cases. These factors are selected conservatively, based on the runout extent of rock avalanches inventoried by Mitchell et al. (2019) and Velardi et al. (2020). The weighting factors consider the probability of exceedance of each runout case. The probability of exceedance (i.e., the chance that a rock avalanche runs out beyond a specific location along a landslide path) decreases with increasing distance from the source.

2.4.2 Individual Life-loss Risk Map

Life-loss risk (individual and group risk) and economic risk are quantified (this paper only presents the individual life-loss risk assessment). The risk assessment is completed at a parcel level. Risks from representative risk scenarios are summed to quantify the total risk.

Individual life-loss risk (*PDI$_j$*) is quantified using Equation 2.

$$PDI_j = \sum_{i=1}^{n} P(H)_i P(S|H)_{i,j} P(T|S)_{i,j} V_{i.j} \quad [2]$$

where $P(H)_i$ is the annual probability of landslide scenario (i); $P(S|H)_{i,j}$ the spatial probability of impact of geohazard scenario (i) at a given parcel (j); $P(T|S)_{i,j}$ the temporal probability of a person occupying a building at parcel (j); and $V_{i,j}$ the probability of fatality (vulnerability) given impact by the estimated hazard intensity.

Temporal probability is estimated based on the primary use of the parcels. For example, the amount of time occupants spend within a home is likely higher than the amount of time occupants spend in school or at work, and consequently the temporal probability for homes is higher. Criteria used to estimate the vulnerability of persons within buildings to landslide impact as an indirect consequence of building damage are based on the landslide intensity index (I_{DF}) shown in Equation 3 (Jakob et al. 2012).

$$I_{DF} = d_f \times v^2 \quad [3]$$

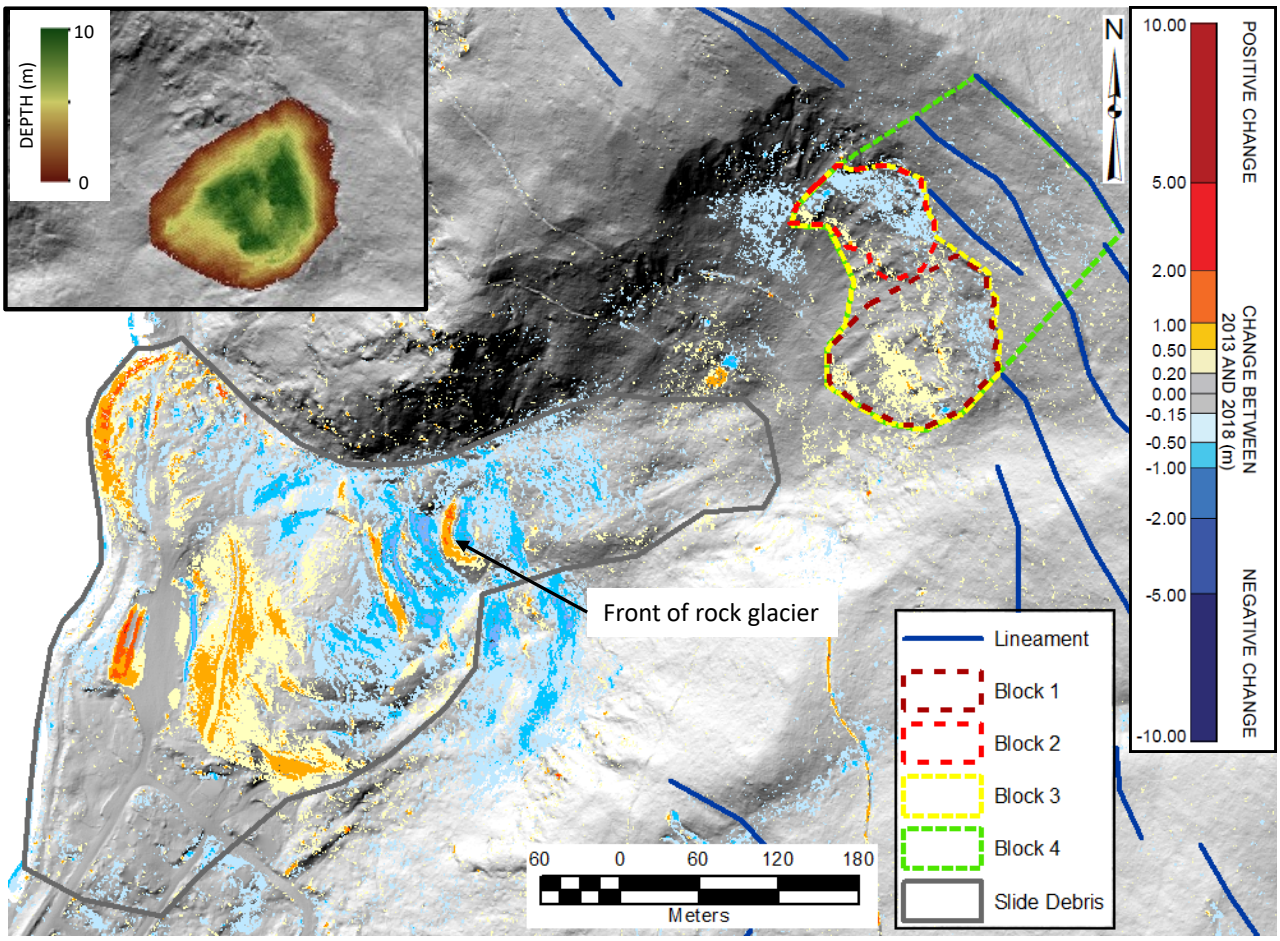

Figure 2. ALS change detection results between 2013 and 2018. Positive model differences (in metres) can be interpreted as material accumulation or bulging, and negative model differences as a loss of material (material removal, erosion or slumping). Zones of positive model difference are coloured yellow to red; zones of negative model difference are coloured light to dark blue. If the calculated change between the two datasets is less than the LoD, the area is coloured grey. Inset map illustrates the depth (in metres) of the failure surface below Block 1 scenario estimated based on the SLBL analysis.

3 HAZARD CHARACTERIZATION RESULTS

3.1 Landslide Source Volume & Failure Probability

Four block scenarios are identified based on the ALS change detection results. Unstable blocks are characterized by a combination of negative change at the top of the blocks and positive change on the lower parts (Figure 2).

The volume estimations using the SLBL (Table 1) are constrained by both geomorphological mapping (e.g., tension cracks, escarpments, lineaments) and the change detection results. The top of Blocks 1 and 2 corresponds to a 200 m tension crack, which exhibits signs of recent movement, including disturbed vegetation, exposed soil horizons, stretched roots and tension-split tree trunks. Block 3 corresponds to a combination of Blocks 1 and 2. Block 4 extends to a lineament located near the ridge.

Annual hazard probability for each block scenario, i.e., the likelihood of failure of the entire block scenario (as opposed to failures in a fragmental manner) is provided in Table 1. For Blocks 1 and 2, estimates are constrained by aerial and historical photograph observations, which clearly show that Blocks 1 and 2 have been moving for decades; and by survey stake measurements along the 200 m tension crack, which indicate that Block 1 has been moving at rates between 2 and 14 cm per year since at least 2006 (Brideau et al. 2012; 2015).

The annual hazard probability for Block 3 is considered smaller, because Blocks 1 and 2 appear relatively independent from each other (Figure 2) and are therefore more likely to fail independently. The order of magnitude probability for Block 3 is consistent with the estimated age of the pre-historic Moosehide Landslide (1,740 BP) by Hughes (1979). Block 4 is defined based on negative change indicators along lineaments near the ridge (Figure 2). However, field observations at these lineaments do not confirm signs of activity (e.g., cracking, disturbed trees) and consequently the annual hazard probability for Block 4 is estimated at less than 0.0001.

Table 1. Block scenario volumes and annual hazard probability range.

Block Scenario	Block Volume m^3	Annual Hazard Probability
Block 1	52,000	0.001 – 0.01
Block 2	33,000	0.001 – 0.01
Block 3	93,000	0.0001 – 0.001
Block 4	245,000	0.00001 – 0.0001

3.2 Permafrost Degradation

In the Dawson City area, permafrost has been degrading proportional to increases in air temperatures. This has resulted in thaw of interstitial ice and an increase in active layer thickness (Laxton & Coates 2011). Since 1948 the average annual temperature in the Yukon has increased by 2 to 3°C (ECCC 2020).

Geothermal modelling using conservative, literature-based assumptions on material properties and boundary conditions indicates that the current active layer thickness may increase by approximately 10% in response to a 1°C warming in air temperature, compared to the 1991-2010 Climate Normals, which is estimated to be reached by 2024 (RCP8.5 projection on climatedata.ca), and by about 30% if the air temperature warms by 2°C (estimated by 2042). The simulation results project that once air temperature increases between 2°C and 3°C from the 1981-2010 Climate Normals, permafrost would be in disequilibrium with the climate at all depths and permafrost would progressively degrade. During this period, the thaw depth would be expected to exceed the freezing depth causing development of a supra-permafrost talik and the thaw depth to the permafrost table would increase until permafrost has disappeared. The main consequence related to landslide mobility is that permafrost degradation results in an increase in material availability for material entrainment along the Moosehide Landslide deposit.

The increase in air temperature of up to 3 ℃ is not expected to alter the volume of the source zone since the depths of the potential failure surfaces are deeper than the zones ultimately affected by changes in air temperature. In addition, Bonnaventure et al. (2012) suggest that permafrost probability in the Dawson region decreases on south-facing slopes and with elevation above the valley bottoms due to inverted surface lapse rates, which promote cold air drainage to valley bottom during winter months.

Projected increases in total annual precipitation, especially during the summer months, will further change the hydrology of the Moosehide Slide area. Increases in runoff due to higher snowmelt amounts and rates as well as increases in summer rainfall may increase pore water pressures within the rock mass. This may, over time, lead to an increase in the probability of rock avalanche initiation. This time-dependent change is not included in this risk assessment as it cannot be currently quantified reliably.

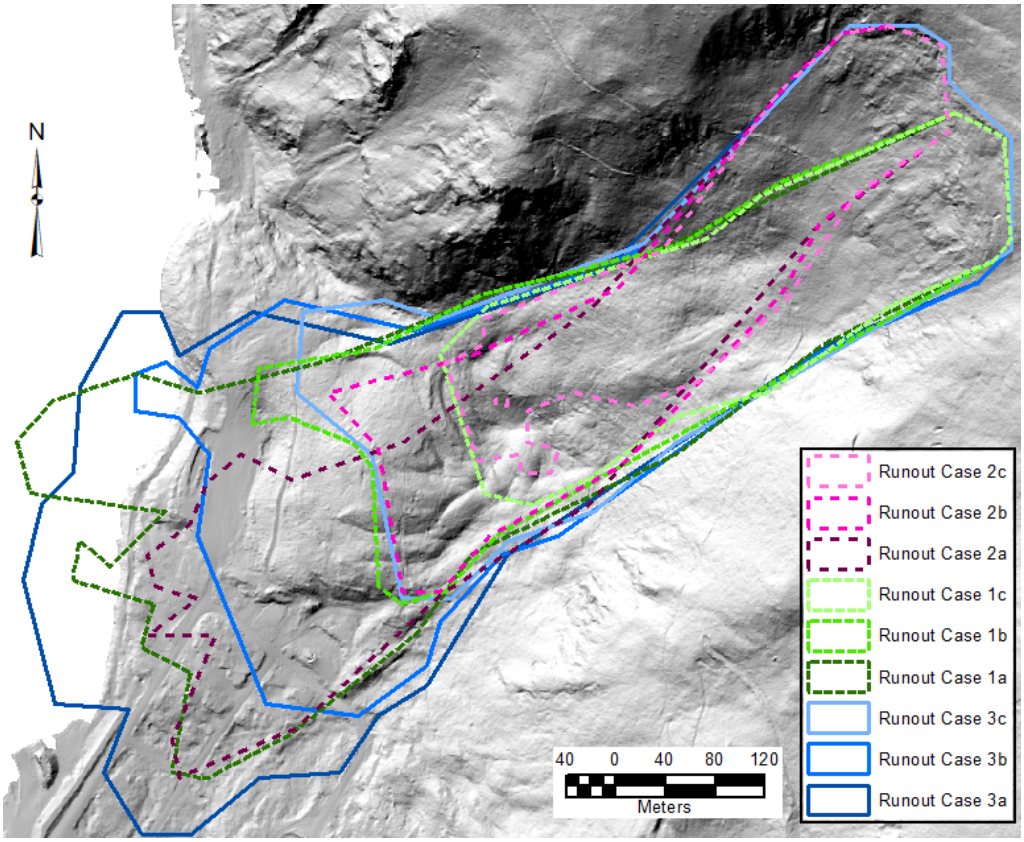

Figure 3. Summary of runout cases assessed.

3.3 Landslide Runout Extent and Intensity

A large dataset of calibrated landslide runout cases (Aaron & McDougall 2019) from a variety of environments are used to establish plausible ranges of parameter inputs for runout modelling (Table 2). The results show that for some runout cases the north end of Dawson City could be impacted (Figure 3). The model results are very sensitive to the initial rock avalanche volume. Comparing results with the same rheology parameters but different source volumes indicates that runout length increases by approximately 25% to 40%, and the impact area increases by approximately 40% to 70% using a larger source volume. Note that in the runout modelling, the volume of the source is increased by approximately 25% to account for material dilation, the volume expansion from the in-place rock fracturing resulting in void space between the fragments (Hungr & Evans 2004).

Material entrainment increases the mobility of the modelled rock avalanche scenarios. However, even with conservative entrainment rates (entrainment ratio ~ 1, i.e., resulting in a final volume approximately twice that of the source volume), the maximum modelled erosion depth is less than the active layer under current conditions. Therefore, no change in the extent of the runout is expected in response to additional permafrost degradation.

Table 2. Runout cases, associated runout parameters and weightings (for composite hazard map generation).

Block Scenario	Runout Case	Runout Parameter			Weighting
		Friction Angle φ (°)	Friction Coeff. f	Turbulence Coeff. ξ	
Block 1	1a	20	n/a	n/a	0.1
	1b	25	n/a	n/a	0.2
	1c[1]	30	n/a	n/a	0.7
Block 2	2a	20	n/a	n/a	0.1
	2b	25	n/a	n/a	0.2
	2c[1]	30	n/a	n/a	0.7
Block 3	3a	n/a	0.1	500	0.1
	3b	n/a	0.2	500	0.2
	3c	n/a	0.3	500	0.7
Block 4	4a[2]	n/a	0.1	500	0.1
	4b[2]	n/a	0.2	500	0.2
	4c[2]	n/a	0.3	500	0.7

[1]scenarios not considered in the risk assessment because runout does not extend to existing development.

[2]scanarios associated with Block 4 not considered in the hazard or risk assessment because annual hazard probability is less than 0.0001.

4 HAZARD AND RISK MAPPING

A key component of the landslide risk management process is the communication of both landslide hazard and risk to the public and decision makers. In this section, we compare two types of maps that were generated for the Moosehide Slide. Note that secondary hazards, such as the impact wave of a rock avalanche reaching the Yukon River, are not included in the maps. Similarly, ongoing deformation of the rock glacier / earthflow, featured as alternating zones of positive and negative changes in Figure 2, presents risks to development along the landslide's margins. These risks are largely of economic nature (mostly slow cracking of foundations, differential settling) rather than life-loss and are not included in these maps.

4.1 Composite Hazard Map

The composite hazard map provides a quantitative estimate of landslide intensity combined with respective probabilities, allowing zonation of the landslide from low to very high hazard. The map allows identification of zones where risk may be unacceptable, without the need for a detailed risk assessment. Figure 4 shows that 18 existing buildings are located within the zones with moderate to very high hazard.

The zones on the map may be subject to specific land-use prescriptions, covenants, bylaws or other limiting clauses for both existing and proposed development. Composite landslide hazard maps are an emerging standard in British Columbia. Other countries, such as Switzerland and Norway, have already integrated landslide hazard zonation in land-use planning (Lateltin 1997; Kristensen et al. 2020).

4.2 Individual Life-loss Risk Map

The result of the individual life-loss risk assessment (Figure 5) is that 14 existing developments are exposed to a risk exceeding 0.0001, and one existing development is exposed to a risk exceeding 0.00001. The risk tolerance thresholds of 0.0001 and 0.00001 for existing and proposed development, respectively, are those adopted by some jurisdictions in Canada (e.g., Town of Canmore 2016; DNV 2018; Cowichan Valley Regional District, 2019).

5 LANDSLIDE RISK MANAGEMENT

Options to mitigate the risk associated with a rock avalanche are limited, due to the magnitude of the failure process. A near real-time monitoring program and early warning system, combined with a response protocol, is recognized as a life-loss risk management measure for existing development where physical mitigation may not be possible or cost-prohibitive (e.g., Loew et al. 2017; Kristensen et al. 2020; Strouth & McDougall 2022). It is based on the experience that slope movement typically accelerates prior to failure, allowing for evacuating buildings at risk.

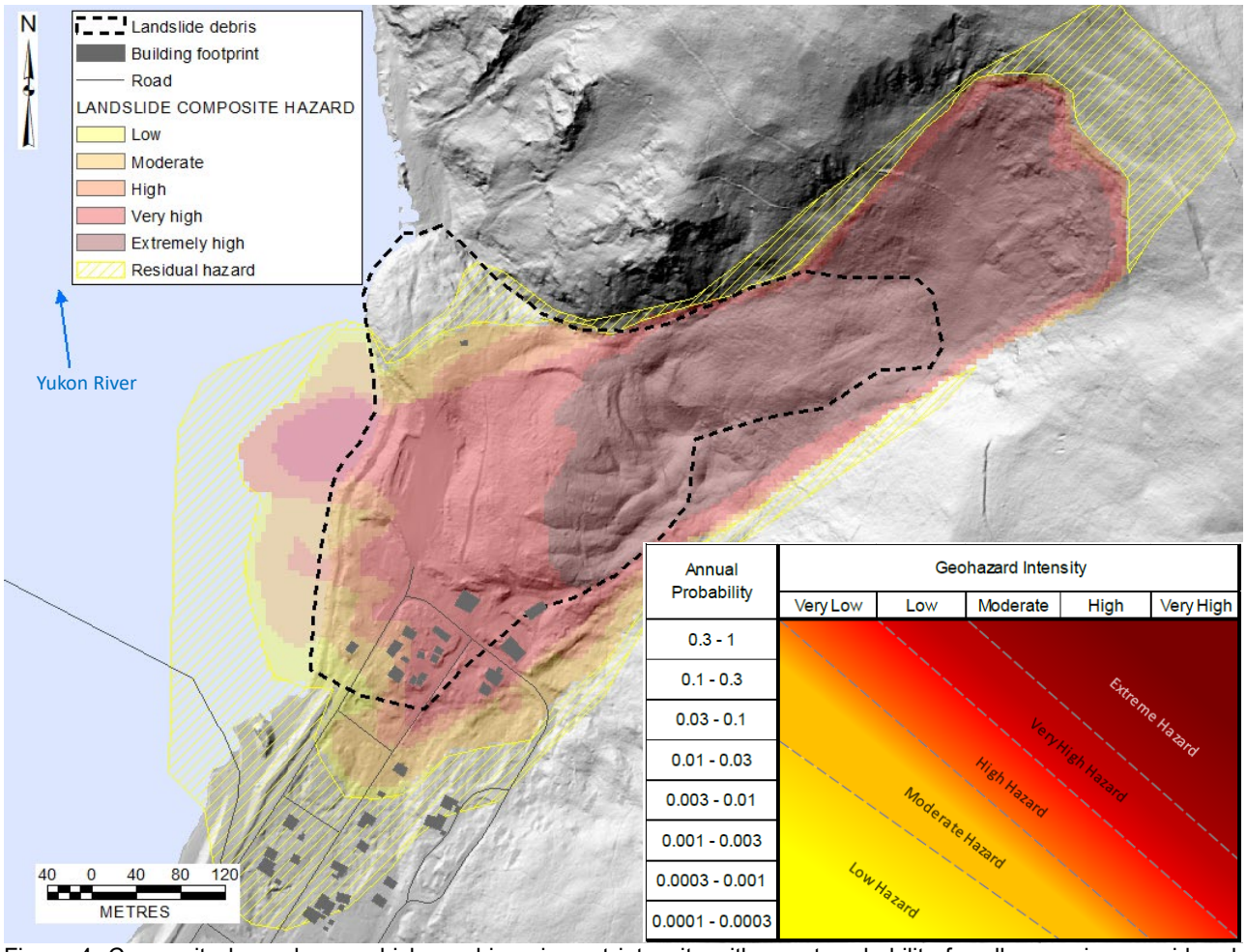

Figure 4. Composite hazard map which combines impact intensity with event probability for all scenarios considered. The inset figure shows a matrix with flow intensity on the horizontal axis and annual hazard probability on the vertical axis.

A near real-time monitoring program is being considered at the Moosehide Slide by the Yukon government and City of Dawson officials. It is based on the installation of GNSS units, extensometers, tiltmeters and an automated weather station for long-term monitoring of the Moosehide Slide headscarp area (Arenson, 2022). The implementation of this program focuses on identifying trends in long-term movement of the landslide and potential acceleration. If landslide acceleration is confirmed, the near real-time monitoring program would likely need to be supplemented, for example, by ground-based InSAR (GB InSAR) for real-time data collection.

Once the monitoring instruments are installed, the setup, data validation and development of an understanding of the slope deformation will occur over approximately one year. At the end of this period, the monitoring program may be integrated in an early warning system, consisting of pre-defined alert levels, associated with an emergency response plan to evacuate individuals at risk to a safe location if a pre-defined warning level is reached and a rock avalanche is considered to occur imminently.

The proposed near real-time monitoring program is part of a larger scale monitoring program for the Moosehide Slide, which includes ALS change detection analysis at regular intervals to detect potential signs of retrogression outside of the main unstable block scenarios.

6 ACKNOWLEDGMENT

The work presented in this paper is funded by the Yukon Government (Yukon Geological Survey and Community Services).

7 REFERENCES

Aaron, J. and McDougall, S. 2019. Rock avalanche mobility: the role of path material. *Engineering Geology*, 257: 1-9.

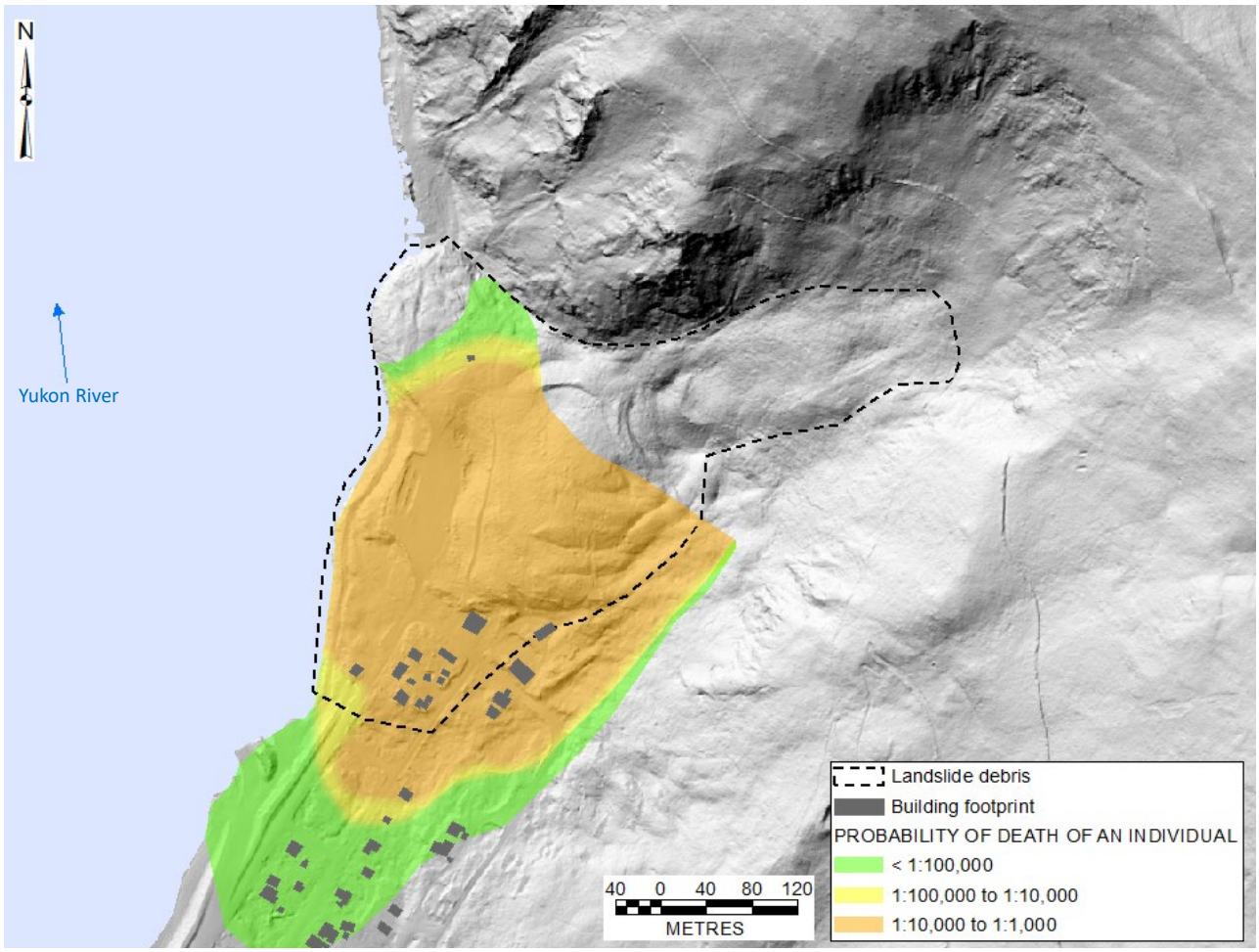

Figure 5. Individual life-loss risk map.

Abellan, A., Jaboyedoff, M., Oppikofer, T. and Vilaplana, J.M. 2009. Detection of millimetric deformation using a terrestrial laser scanner: experiment and application to a rockfall event. *Natural Hazards and Earth System Sciences*, 9: 365-372.

Arenson, L. 2022. Geohazard management in permafrost regions, Geohazard 8 Conference, Québec City, Canada, 9 p.

Bonnaventure, P.P., Lewkowicz, A.G., Kremer, M. and Sawada, M. 2012. A regional permafrost probability model for the southern Yukon and northern British Columbia, Canada. *Permafrost and Periglacial Processes*, 23: 52-68.

Brideau, M.-A., Stead, D., Roots, C. and Orwin, J. 2007a. Geomorphology and engineering geology of a landslide in ultramafic rocks, Dawson City, Yukon, *Engineering Geology*, 89: 171-194.

Brideau, M.-A., Stead, D., Stevens, V., Roots, C., Lipovsky, P. and VonGaza, P. 2007b. The Dawson City landslide (Dawson map area NTS 116B/3), central Yukon. In: D.S. Emond, L.L. Lewis and L.H. Weston (eds.), Yukon Exploration and Geology 2006, Yukon Geological Survey, 123-137.

Brideau, M.-A., Stead, D., Roots, C. and Lipovsky, P. 2012. Ongoing displacement monitoring at the Dawson City landslide (Dawson map area NTS 116B/3). In: K.E. MacFarlane and P.J. Sack (eds.), Yukon Exploration and Geology 2011, Yukon Geological Survey, 17-26.

Brideau, M.-A., Bevington, A. Lewkowicz, A. and Stead, D. 2015. Engineering geology, electrical resistivity tomography and displacement monitoring of the Dawson City landslide, Yukon, GeoQuébec 2015 Conference, Québec City, Canada, 8 p.

Corominas, J. 1996. The angle of reach as a mobility index for small and large landslides. *Canadian Geotechnical Journal*, 33: 260-271.

Cowichan Valley Regional District. 2019. Natural Hazard Risk Tolerance Policy. Duncan, BC.

District of North Vancouver [DNV]. 2018. Our Official Community Plan for a Sustainable Future (Bylaw 7900). North Vancouver, BC.

Environment and Climate Change Canada [ECCC]. 2020. Canadian Climate Normals 1981-2010 Station Data. https://climate.weather.gc.ca/climate_normals/index_e.html (data extracted on February 12, 2020).

Green, L.H. 1972. Geology map, Dawson, Yukon Territory. Map 1284A, scale 1:250,000. Geological Survey of Canada, Ottawa.

Hughes, O.L. 1979. Analysis undertaken by the Radiocarbon Laboratory, Terrain Sciences Division, Geological Survey of Canada.

Hungr, O. and Evans, S. 2004. Entrainment of debris in rock avalanches: an analysis of a long run-out mechanism. *GSA Bulletin*, 116, B25362: 1-13.

Hungr, O., Leroueil, S. and Picarelli, L. 2014. Varnes classification of landslide types, an update. *Landslides*, 11: 167-194.

Innovmetric 2020. Polyworks Inspector, version IR3. https://www.innovmetric.com/en

Jaboyedoff, M., Baillifard, F., Couture, R., Locat, J. and Locat, P. 2004. Toward preliminary hazard assessment using DEM topography analysis and simple mechanic modeling. In: W.A. Lacerda, M. Ehrlich, A.B. Fontoura. and A. Sayo (eds.), Landslides Evaluation and Stabilization, Belkema, 191-197.

Jaboyedoff, M., Chigira, M., Arai, N., Derron, M.-H., Rudaz, B. and Tsou, C.-Y. 2019. Testing a failure surface prediction and deposit reconstruction method for a landslide cluster that occurred during Typhoon Talas (Japan). *Earth Surface Dynamics Discussions*, 7: 439-458.

Jakob, M., Stein, D. and Ulmi, M. 2012. Vulnerability of buildings to debris flow impact. *Natural Hazards*, 60(2): 241-261.

Jakob, M., Davidson, S., Bullard, G., Busslinger, M., Collier-Pandya, B., Grover, P. and Lau, C.-A. 2022. Debris-Flood Hazard Assessments in Steep Streams. *Water Resources Research*. In print.

Kristensen, L., Pless, G., Blikra, L.H. and Anda, E. 2020. Management and monitoring of large rockslides in Norway. Keynote Lecture, ISRM International Symposium Eurock, Trondheim, Norway.

Lateltin, O. 1997. Recommendations prise en compte des dangers dus aux mouvements de terrain dans le cadre des activités de l'aménagement du territoire, OFAT, OFEE and OFEFP, Switzerland, 42 pp.

Lato, M.J., Hutchinson, D.J., Gauthier, D., Edwards, T. and Ondercin, M. 2015. Comparison of ALS, TLS and terrestrial photogrammetry for mapping differential slope change in mountainous terrain. *Canadian Geotechnical Journal*, 52(2): 129-140.

Laxton, S. and Coates, J. 2011. Geophysical and borehole investigations of permafrost conditions associated with compromised infrastructure in Dawson and Ross River, Yukon. In: K.E. MacFarlane, L.H. Weston, and C. Relf (eds.), Yukon Exploration and Geology 2010. Yukon Geological Survey.

Loew, S., Gschwind, S., Gischig, V., Keller-Signer, A. and Valenti, G. 2017. Monitoring and early warning of the 2012 Preonzo catastrophic rockslope failure. *Landslides*, 14: 141-154.

McDougall, S. 2017. 2014 Canadian Geotechnical Colloquium: Landslide runout analysis – current practice and challenges. *Canadian Geotechnical Journal*, 54: 605-620

McDougall, S. and Hungr, O. 2004. A model for the analysis of rapid landslide motion across three-dimensional terrain. *Canadian Geotechnical Journal*, 41: 1084-1097.

Mitchell, a., McDougall, S., Nolde, N., Brideau, M.-A., Whittall, J. and Aaron, J.B. 2019. Rock avalanche runout prediction using stochastic analysis of a regional dataset, *Landslides*, 17: 777-792.

Oppikofer, T., Jaboyedoff, M., Blikra, L., Derron, M.-H. and Metzger, R. 2009. Characterization and monitoring of the Aknes rockslide using terrestrial laser scanning. *Natural Hazards and Earth System Sciences*, 9: 1003-1019.

Sokolowski, D. 2020. Ëdhä dädhëchą (movie), https://en.sgi-ontherocks.it/N323/edha-dadhecha.html

Strouth, A. and McDougall, S. 2022. Individual risk evaluation for landslides: key details. *Landslides*, 19:977-991.

Town of Canmore 2016. Canmore Municipal Development Plan (Bylaw 2016-03). Canmore, Alberta.

VanDine, D.F. 2012. Risk Management – Canadian Technical Guidelines and Best Practices Related to Landslides. Geological Survey of Canada, Open File 6996, 8 p.

Velardi, G., Hermanns, R.L., Penna, I. and Böhme, M. 2020. Prediction of the reach of rock slope failures based on empirical data from Norway. ISRM International Symposium Eurock, Trondheim, Norway.